JOURNAL OF SOLID STATE CHEMISTRY **123,** 129–139 (1996)
ARTICLE NO. 0161

$Na_4Co_3(PO_4)_2P_2O_7$, a New Sodium Cobalt Phosphate Containing a Three-Dimensional System of Large Intersecting Tunnels

F. Sanz,* C. Parada,* U. Amador,† M. A. Monge,†‡,[1] and C. Ruiz Valero†,‡

*Departamento de Química Inorgánica, Facultad de Ciencias Químicas, Universidad Complutense, E-28040 Madrid, Spain; †C.A.I. de Difracción de Rayos-X, Facultad de Ciencias Químicas, Universidad Complutense, E-28040 Madrid, Spain; ‡Instituto de Ciencias de Materiales, C.S.I.C.,C/Serrano 113, E-28006 Madrid, Spain

Received August 7, 1995; in revised form January 22, 1996; accepted January 25, 1996

Single crystals of the new Co(II) phosphate $Na_4Co_3(PO_4)_2P_2O_7$ have been isolated and their structure has been determined by X-ray diffraction techniques. This compound crystallizes in the orthorhombic noncentrosymmetric space group $Pn2_1a$ with $a = 18.046(5)$ Å, $b = 6.533(2)$ Å, $c = 10.536(2)$ Å, and $Z = 4$. The structure consists of infinite layers with composition $(Co_3P_2O_{13})_\infty$ parallel to the bc plane. Interlayer linkages are made via P–O–P bridges of the pyrophosphate groups in such a way that large tunnels extending along the [010] and [001] directions occur between two neighboring sheets. Besides, there also exist channels along the [100] direction crossing the $(Co_3P_2P_{13})_\infty$ layers. A complex scheme of tunnel intersections gives rise to the formation of a three-dimensional channel network which hosts the sodium cations.

INTRODUCTION

The phosphates of transition metals form a huge family of compounds showing many interesting properties (1). Most of them are characterized by a mixed framework built up from MO_6 octahedra and PO_4 tetrahedra defining a great variety of polyhedral connectivities. The association of metallic or semi-metallic rows or layers of MO_6 octahedra with insulating PO_4 rows or layers gives rise to original physical properties. Moreover, it is well known that many phosphates are good ionic conductors, mainly those showing the NASICON-type structure (2). Due to these reasons, a great effort, during the past years, has been devoted to the study of mixed transition-metal phosphates. Among them, those containing titanium, vanadium, molybdenum, tungsten, or niobiom have been widely studied (1 and references therein) while the Co–P–O system remains relatively poorly explored. To our knowledge, only a limited number of phosphates of cobalt have been reported so far (3–14). Most of them are hydro- or hydroxyphosphates and there are few examples of pyrophosphate-containing phases (9–14).

In this paper we present the synthesis and the crystal structure determination of the new sodium cobalt phosphate $Na_4Co_3(PO_4)_2P_2O_7$. The structure of this compound is built up from corner- and edge-sharing between CoO_6 octahedra and PO_4 and P_2O_7 groups giving rise to a polyhedral connectivity which produces large tunnels running along the three main crystallographic directions [100], [010], and [001]. As a consequence of a complex scheme of tunnel intersections, a three-dimensional channel network occurs, the sodium cations being located within those tunnels.

EXPERIMENTAL

1. Crystal Growth

Crystals of the title compound were grown by melting a mixture of analytical grade $Na_2CO_3 \cdot 10H_2O$, $Co(acac)_3$, and $NH_4H_2PO_4$ in a molar ratio Na/Co/P = 3/2/3. After grinding, the mixture was held in a zirconia crucible and slowly heated to 983 K. The batch was kept at this temperature for 2 h to homogenize the melt, being then slowly cooled down to 733 K at a rate of 50°/h and from this value to room temperature at 100°/h.

2. Data Collection

A purple-colored prismatic-shaped crystal was mounted in a Nonius CAD-4 diffractometer to be used for the structure determination. Table 1 collects the main crystal data and refinement parameters for $Na_4Co_3(PO_4)_2P_2O_7$.

A graphite-monochromated Mo$K\alpha$ ($\lambda = 0.71069$ Å) beam was used for the data collection.

The unit cell parameters were determined by least-square refinement of the 2θ values of 25 strong well centered reflections in the range $18° < 2\theta < 31°$.

Raw data were corrected for Lorentz and polarization effects. Scattering factors for neutral atoms and anomalous

[1] To whom correspondence should be addressed.

0022-4596/96 $18.00

TABLE 1
Crystal, Measurement, and Refinement Parameters for $Na_4Co_3(PO_4)_2P_2O_7$

	Crystal data
Crystal dimensions (mm^3)	$0.25 \times 0.2 \times 0.1$
Formula	$Co_3P_4Na_4O_{15}$
Formula weight (g mol^{-1})	632.6
Crystal system	Orthorhombic
Space group	$Pn2_1a$
Cell dimensions	
a (Å)	18.046(5)
b (Å)	6.533(2)
c (Å)	10.536(2)
Z	4
V ($Å^3$)	1242.1(5)
ρ_{calcd}(g cm^{-3})	1.38
	Data collection
Radiation	Mo$K\alpha$ (λ = 0.71069 Å)
Temperature (°K)	295
Scan technique	$\omega/2\theta$
2θ range (°)	1 − 60
Data collected	(−25, 0, 0) to (25, 9, 14)
Decay	≤1%
Unique data (after merging)	1958
Observed reflections $I > 2\sigma(I)$	1791
R_{int}, %	4.2
$F(000)$	1220
μ(Mo$K\alpha$)(cm^{-1})	46.9
	Structure solution and refinement
Agreement factors	$R = 0.039$, $R_w = 0.046$
Weighting scheme	$w = w_1w_2$, $w_1 = 1/(a + b\|F_o\|)^2$, $w_2 = 1/(c + d \sin\theta/\lambda)^2$
	$a = 1.31$, $b = 0.012$, $\|F_o\| < 450$
	$c = 4.09$, $d = -8.68$, $0 < \sin\theta/\lambda < 0.44$
	$c = -0.61$, $d = 2.61$, $0.44 < \sin\theta/\lambda < 0.80$
Maximum and average shift/error	0.04, 0.009
Absorption correction range	0.96–1.02
Maximum residual ($eÅ^{-3}$)	1.4

dispersion correction for Co and P atoms were taken from ''International Tables for X-Ray Crystallography'' (15).

3. Structure Determination

The systematic absence conditions in the reduced data ($hk0$, $h = 2n$; $0kl$, $k + l = 2n$; $h00$, $h = 2n$; $0k0$, $k = 2n$; and $00l$, $l = 2n$) were consistent with space groups $Pnma$(No. 62) and $Pn2_1a$ (non standard setting of S.G. $Pna2_1$, No. 33). An initial model of the crystal structure was developed in the centrosymmetric space group $Pnma$ with heavy-atom positions (Co, P, and Na) located using the direct-methods program MULTAN80 (16). However, along the data refinement, it was apparent that these heavy atoms were not centrosymmetrically arranged. Thus, after trying the centrosymmetric space group, the structure was solved in the noncentrosymmetric group $Pn2_1a$. The positions of the oxygen atoms were obtained by Fourier synthesis. An empirical absorption correction (17) was applied at the end of the isotropic refinement; the agreement factors before and after the application of this correction were $R = 0.059$, $R_w = 0.068$ and $R = 0.049$, $R_w = 0.060$, respectively. In order to prevent bias on ΔF vs F_o or sin θ/λ, weights were assigned using the weighting scheme and the coefficients, calculated by the program PESOS (18), collected in Table 1. Full-matrix least-squares refinement with anisotropic thermal parameters for all the atoms led to agreement factors $R = 0.039$ and $R_w = 0.046$. The maximum and average shift-to-error ratios were 0.04 and 0.009, respectively, while the maximum residual electron density near the Co(1) atom was 1.4 $eÅ^{-3}$. Most of the calculations were carried out with the X-RAY80 program (19).

4. Supplementary Characterization

In order to confirm some important points of the crystal structure of $Na_4Co_3(PO_4)_2P_2O_7$ chemical analysis and magnetic susceptibility measurements were performed. Chemical analyses of several crystals were carried out by the Inductively Coupled Plasma technique using a Jovin Yvon

TABLE 2
Atomic Parameters for $Na_4Co_3(PO_4)_2P_2O_7$

Atom	*x/a*	*y/b*	*z/c*	U_{eq}[a] (Å^2)
Co(1)	0.33410(4)	0.10080(1)	0.5028(1)	50(2)
Co(2)	0.13900(4)	−0.4099(2)	0.4948(1)	49(2)
Co(3)	0.24290(5)	0.3226(2)	0.7423(1)	59(2)
P(1)	0.2925(1)	−0.4015(3)	0.5015(1)	39(4)
P(2)	0.1791(1)	0.0881(3)	0.4864(1)	38(4)
P(3)	0.5680(1)	0.4554(3)	0.7368(1)	39(4)
P(4)	0.4486(1)	0.1469(3)	0.7275(1)	54(4)
Na(1)	0.4934(2)	0.8190(5)	0.9768(3)	116(7)
Na(2)	0.2955(2)	−0.1480(6)	0.7472(3)	150(8)
Na(3)	0.3941(2)	−0.5719(6)	0.2635(3)	169(8)
Na(4)	0.4620(2)	−0.3262(6)	0.5410(3)	177(8)
O(1)	0.2362(3)	−0.4397(7)	0.6118(4)	51(12)
O(2)	0.3440(3)	−0.5803(8)	0.4764(5)	105(13)
O(3)	0.3381(3)	−0.2116(8)	0.5351(5)	75(13)
O(4)	0.2403(3)	−0.3714(8)	0.3855(4)	65(12)
O(5)	0.2320(2)	0.1137(9)	0.6031(4)	74(12)
O(6)	0.1270(3)	−0.0919(8)	0.5122(5)	99(13)
O(7)	0.2340(3)	0.0548(8)	0.3743(5)	68(12)
O(8)	0.1351(3)	0.2829(9)	0.4573(5)	96(13)
O(9)	0.4870(3)	0.3696(8)	0.6978(5)	83(12)
O(10)	0.5575(3)	0.5666(8)	0.8628(4)	91(12)
O(11)	0.6222(3)	0.2804(8)	0.7430(5)	80(12)
O(12)	0.5839(2)	0.6058(9)	0.6303(4)	93(11)
O(13)	0.4566(2)	0.1119(9)	0.8694(4)	82(11)
O(14)	0.3687(3)	0.1714(9)	0.6889(4)	107(12)
O(15)	0.4904(3)	−0.0032(10)	0.6475(5)	136(14)

[a] $U_{eq} = 1/3(\Sigma_i \Sigma_j U_{ij} a_i^* a_j^* \mathbf{a}_i \mathbf{a}_j)10^4$.

JY-70 plus apparatus. Magnetic susceptibility measurements in the temperature range from 298 to 77 K were performed using an ASMI magnetometer (minimum magnetic field 14 KG with HdH/dz = 29 KG^{2}cm^{-1}).

RESULTS AND DISCUSSION

Applying the crystal growth procedure explained in the Experimental section, many purple-colored prismatic-shaped crystals with mm-sized edges were obtained on the surface of the cake melt. The composition determined by the refinement of the X-ray diffraction data was confirmed by chemical analysis. The calculated and experimental molar ratios Na/Co/P are 4/3/4 and (4.1 ± 0.1)/(3.0 ± 0.1)/(3.7 ± 0.2), respectively.

Final atomic parameters are collected in Tables 2 and 3; Table 4 shows some selected geometrical information.

The three crystallographically distinct cobalt atoms exhibit the normal octahedral coordination, with average Co–O distances of 2.122(5), 2.126(5), and 2.154(5) Å for Co(1), Co(2), and Co(3), respectively. These distances agree with that corresponding to the radius of a divalent high-spin-six-coordinated cobalt cation (20). From the magnetic susceptibility measurements, an effective magnetic moment per cobalt ion of μ_{eff} = 5.52(1) μ_BM was obtained. This value is in agreement with those previously found in other compounds for high-spin-Co^{2+} cations (21). It is worth noting that the $Co(3)O_6$ octahedron is rather irregular with a large Co(3)–O(14) distance. As it will be shown, this is a consequence of the location of Co(3) in the structure.

Due to the corner- and edge-sharing (see below) the two monophosphate groups show a distorted tetrahedral environment, with average P–O distances P(1)–O = 1.541(5) Å and P(2)–O = 1.546(5) Å.

The pyrophosphate groups take up an alternated configuration, with the O(9) as bridging oxygen. As expected (22), the bridging P–O bonds are longer than the terminal ones. However, the P–O_{bridge} distances found in $Na_4CO_3(PO_4)_2P_2O_7$ are unusually long, P(3)–O(9) = 1.619(5) Å and P(4)–O(9) = 1.642(5) Å, while in $Co_2P_2O_7$ (14) P–O_{bridge} = 1.582 Å. Similar values (1.645 and 1.625 Å) have been reported by Lightfoot *et al.* in $K_2Co_3(P_2O_7)\cdot 2H_2O$ (11). These authors claimed that those long P–O_{bridge} bonds are due to the bending of the pyrophosphate (P–O_{bridge}–P = 127.17°) as a consequence of acting as bidentate ligand in their compound. This is not the case in our material, although the P(3)–O(9)–P(4) angle (129.7°) is not closer

TABLE 3
Anisotropic Thermal Parameters[a] for $Na_4Co_3(PO_4)_2P_2O_7$

Atom	U_{11}	U_{22}	U_{33}	U_{12}	U_{13}	U_{23}
Co(1)	42(3)	51(4)	58(3)	0(4)	15(3)	−2(3)
Co(2)	38(3)	48(4)	61(3)	3(4)	4(3)	9(3)
Co(3)	96(4)	49(4)	33(3)	−10(4)	−10(3)	6(3)
P(1)	33(6)	49(7)	36(6)	−3(7)	8(5)	14(6)
P(2)	39(6)	33(7)	40(6)	−1(7)	0(5)	−8(6)
P(3)	35(6)	38(7)	46(6)	−10(6)	1(5)	0(6)
P(4)	55(6)	66(7)	41(6)	−26(6)	−7(5)	−3(6)
Na(1)	87(12)	116(14)	145(12)	41(12)	22(11)	17(13)
Na(2)	201(13)	119(15)	129(12)	−4(12)	17(11)	8(12)
Na(3)	183(14)	163(16)	160(14)	4(14)	−2(11)	4(13)
Na(4)	120(13)	236(13)	173(13)	75(13)	−19(11)	−27(14)
O(1)	79(19)	19(21)	54(21)	−10(17)	9(16)	−1(16)
O(2)	100(21)	75(25)	138(22)	71(21)	37(19)	14(19)
O(3)	57(20)	88(25)	79(20)	11(18)	−13(16)	10(19)
O(4)	76(19)	73(23)	45(19)	−41(18)	−23(15)	42(18)
O(5)	43(18)	110(23)	69(19)	25(19)	−2(16)	−28(20)
O(6)	52(19)	71(24)	174(25)	−18(18)	14(17)	14(20)
O(7)	92(20)	35(22)	76(21)	11(18)	35(17)	−13(16)
O(8)	69(21)	93(24)	127(22)	25(18)	−5(17)	−18(20)
O(9)	66(19)	30(21)	152(21)	−7(17)	−17(17)	44(19)
O(10)	83(19)	126(25)	64(18)	−2(19)	−37(15)	−44(19)
O(11)	108(21)	51(22)	82(20)	13(18)	−11(17)	10(18)
O(12)	78(19)	78(21)	121(19)	20(20)	55(16)	68(20)
O(13)	97(19)	98(21)	52(17)	3(19)	−15(15)	40(18)
O(14)	39(19)	202(26)	80(19)	−11(19)	−30(15)	−43(20)
O(15)	127(22)	151(26)	130(22)	12(21)	34(18)	−51(21)

[a] Thermal parameters as $\exp[-2\pi^2 \Sigma_i \Sigma_j (U_{ij} a_i^* a_j^* H_i H_j)]10^4$.

TABLE 4
Selected Interatomic Distances (Å) and Angles (deg) and Polyhedral Edge Lengths (Å) for $Na_4Co_3(PO_4)_2P_2O_7$

Co(1)	O(3)	O(5)	O(7)	O(14)	$O(2^1)$	$O(12^2)$
O(3)	2.070(5)	2.949(7)	3.071(7)	3.031(8)	4.171(8)	3.052(7)
O(5)	89.3 (2)	2.127(4)	2.442(7)	2.655(6)	3.141(7)	4.135(6)
O(7)	89.7 (2)	67.2 (2)	2.279(5)	4.181(7)	3.283(7)	3.304(6)
O(14)	93.0 (2)	77.6 (2)	144.7 (2)	2.108(5)	2.800(8)	3.496(7)
$O(2^1)$	172.9 (2)	95.7 (3)	96.8 (2)	83.2 (2)	2.109(5)	2.677(7)
$O(12^{11})$	95.9 (2)	166.0 (2)	99.7 (2)	114.9 (2)	80.3 (2)	2.040(5)

Co(2)	O(1)	O(4)	O(6)	$O(8^3)$	$O(10^4)$	$O(13^5)$
O(1)	2.153(5)	2.427(6)	3.186(7)	3.044(7)	3.237(6)	4.330(6)
O(4)	68.2 (2)	2.175(5)	3.049(7)	3.046(7)	4.252(6)	3.559(6)
O(6)	97.1 (2)	91.1 (2)	2.096(6)	4.127(8)	2.878(7)	3.575(7)
$O(8^3)$	92.9 (2)	92.3 (2)	170.0 (2)	2.047(6)	2.998(7)	2.866(7)
$O(10^4)$	98.9 (2)	166.5 (2)	86.4 (2)	92.4 (2)	2.106(5)	2.848(6)
$O(13^5)$	177.2 (2)	109.7 (2)	84.6 (2)	85.4 (2)	83.3 (2)	2.178(4)

Co(3)	O(5)	O(14)	$O(1^1)$	$O(11^6)$	$O(4^7)$	$O(7^7)$
O(5)	2.013(5)	2.655(6)	2.920(7)	2.282(7)	3.018(6)	4.104(7)
O(14)	70.3 (2)	2.538(5)	3.582(7)	4.562(7)	2.870(6)	3.677(3)
$O(1^1)$	91.1 (2)	101.3 (2)	2.078(5)	3.149(7)	4.056(7)	2.817(7)
$O(11^6)$	82.5 (2)	148.4 (2)	94.7 (2)	2.202(5)	2.996(7)	3.388(7)
$O(4^7)$	97.8 (2)	77.5 (2)	170.0 (2)	91.0 (2)	1.993(5)	2.789(7)
$O(7^7)$	172.7 (2)	104.5 (2)	84.8 (2)	103.9 (2)	85.9 (2)	2.100(5)

P(1)	O(1)	O(2)	O(3)	O(4)
O(1)	1.564(5)	2.581(7)	2.501(7)	2.427(6)
O(2)	113.9 (3)	1.515(6)	2.489(7)	2.506(7)
O(3)	107.8 (3)	109.7 (3)	1.530(5)	2.587(7)
O(4)	102.1 (2)	109.4 (3)	113.9 (3)	1.556(5)

P(2)	O(5)	O(6)	O(7)	O(8)
O(5)	1.565(5)	2.512(7)	2.442(7)	2.577(7)
O(6)	108.5 (3)	1.530(6)	2.599(7)	2.520(8)
O(7)	102.9 (3)	114.7 (3)	1.557(5)	2.484(7)
O(8)	112.6 (3)	110.8 (3)	107.1 (3)	1.531(6)

P(3)	O(9)	O(10)	O(11)	O(12)
O(9)	1.619(5)	2.509(7)	2.554(7)	2.438(7)
O(10)	105.9 (3)	1.525(5)	2.540(7)	2.509(7)
O(11)	109.6 (3)	113.9 (3)	1.506(5)	2.540(7)
O(12)	101.9 (3)	111.0 (3)	113.6 (3)	1.519(5)

P(4)	O(9)	O(13)	O(14)	O(15)
O(9)	1.642(5)	2.531(7)	2.498(7)	2.494(8)
O(13)	106.3 (3)	1.520(5)	2.508(6)	2.531(7)
O(14)	104.9 (3)	111.9 (3)	1.506(5)	2.513(7)
O(15)	105.1 (3)	114.0 (3)	113.6 (3)	1.498(6)

P(3)–O(9)–P(4)	129.7(3)	P(3)–P(4)	2.952(3)

TABLE 4—*Continued*

	M–M distances (Å) < 3.70 Å		
Co(1)–Co(3)	3.343(1)	Na(2)–Na(3^{15})[b]	3.462(4)
Co(2)–Co(3)	3.657(2)	Na(3)–Na(4)	3.708(5)
Na(1)–Na(3^{12})	3.322(4)	Na(3)–Na(4^{16})	3.553(5)
Na(1)–Na(1^{13})[a]	3.312(5)	Na(4)–Na(4^{17})[c]	3.648(4)
Na(1)–Na(1^{14})[a]	3.312(5)	Na(4)–Na(4^{18})[c]	3.648(4)
	Na–O distances (Å) < 3.20 Å		
Na(1)–O(10)	2.345(6)	Na(3)–O(2)	2.420(6)
–O(13^1)	2.319(6)	–O(11^2)	2.321(7)
–O(8^7)	2.340(6)	–O(15^2)	2.848(6)
–O(6^8)	2.482(6)	–O(5^5)	3.082(6)
–O(10^9)	2.514(6)	–O(6^5)	2.678(6)
–O(13^9)	2.295(6)	–O(10^{11})	2.848(6)
		–O(12^{11})	2.418(7)
Na(2)–O(1)	2.609(6)	Na(4)–O(2)	2.785(6)
–O(3)	2.399(6)	–O(3)	2.358(6)
–O(5)	2.557(6)	–O(15)	2.444(7)
–O(14)	2.545(7)	–O(9^2)	2.970(6)
–O(4^7)	2.409(6)	–O(15^2)	2.454(6)
–O(7^{10})	2.418(6)	–O(9^3)	2.623(6)
–O(8^{10})	2.584(6)	–O(12^3)	2.433(5)

Symmetry code:

1	$(x, 1 + y, z)$	2	$(1 - x, y - 1/2, 1 - z)$	3	$(x, y - 1, z)$
4	$(x - 1/2, y - 1, -z + 2 + 1/2)$	5	$(1/2 - x, y - 1/2, z - 1/2)$	6	$(x - 1/2, y, 1 + 1/2 - z)$
7	$(1/2 - x, 1/2 + y, 1/2 - z)$	8	$(1/2 + x, 1 + y, -z + 1 + 1/2)$	9	$(1 - x, 1/2 + y, 2 - z)$
10	$(1/2 - x, y - 1/2, 1/2 + z)$	11	$(1 - x, y - 1 - 1/2, 1 - z)$	12	$(1 - x, y + 1/2 + 1, 1 - z)$
13	$(1 - x, y + 1/2, 2 - z)$	14	$(1 - x, y - 1/2, 2 - z)$	15	$(1/2 - x, y + 1/2, z + 1/2)$
16	$(1 - x, y - 1/2, 1 - z)$	17	$(1 - x, y + 1/2, 1 - z)$	18	$(1 - x, y - 1/2, z - 1)$

[a] Distance along B2.
[b] Distance along A1.
[c] Distance along B1.

to linearity. However, like in $Na_2Co_3P_2O_7 \cdot 2H_2O$, the position of the P_2O_7 groups in the structure and the oxygen-sharing with CoO_6 octahedra force their geometry. Thus, in the title compound the $P–O_{bridge}$ bonds are longer than usual while an alternated conformation of the pyrophosphate groups is allowed with the unshared O(15) atoms pointing toward large tunnels occurring in the structure. A similar situation was found in $Na_2CoZr(P_2O_7)_2$ (12). In these cases these terminal oxygen atoms play a particular role in the structure since they are not involved in the structure framework. In this connection it is worth pointing out that, when pyrophosphate groups are condensed with CoO_6 octahedra to build up a layer, they are arranged in an eclipsed or quasi-eclipsed conformation (11, 13). However, if the P_2O_7 groups act as bridges linking parallel layers, like in the title compound, an alternated conformation is allowed.

There are four crystallographically independent sodium atoms in the structure. Three of them are seven-coordinated and one (Na(1)) is octahedrically surrounded by six oxygen atoms. The Na–O distances range from 2.295(6) to 3.082(6) Å, the average value being 2.37(6) Å.

As mentioned before, one of the main features of the structure of $Na_4Co_3(PO_4)_2P_2O_7$ is the existence of infinite layers with composition $(Co_3P_2O_{13})_\infty$ parallel to the *bc* plane. Interlayer linkages are made via P(3)–O(9)–P(4) bridges of the pyrophosphate groups (see Figs. 1 and 2).

Like in other phosphates (1 and references therein), it is possible to describe the structure as built up from simple structural units. Thus, one $(Co_3P_2O_{13})_\infty$ layer consists of alternating infinite double chains of composition $(Co_2P_2O_{13})_\infty$ and cobalt rows running along the *b* axis stacked in the [001] direction (see Fig. 3).

It is quite common to find phosphates in which simple chains of alternating corner-sharing MO_6 octahedra and PO_4 tetrahedra are present. However, to our knowledge, few examples of phosphates showing double chains have been reported so far (7). In the structure of $NaCo_3$

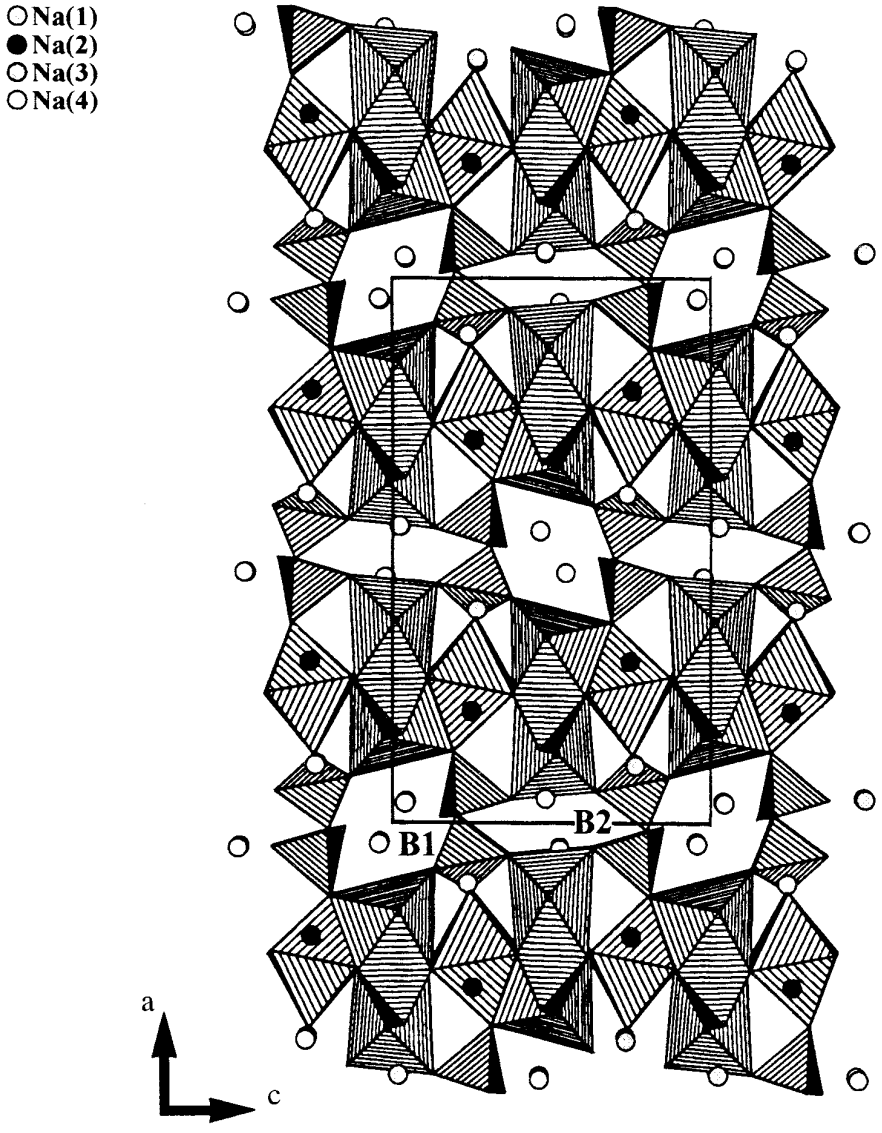

FIG. 1. Polyhedral view down [010] of the structure of $Na_4Co_3(PO_4)_2P_2O_7$ showing two types of 6-ring tunnels, B1 and B2. The four crystallographically distinct sodium atoms are drawn with different shading.

$(PO_4)(HPO_4)$, determined by Lii *et al.* (7), the double chains are built up from CoO_6 octahedra which share edges with other CoO_6 and are joined to PO_4 groups by corner-sharing. The double chains in the title compound (shown in Fig. 3a) consist of $Co(1)O_6$ octahedra which share the apical oxygen atoms O(2) and O(3) with two $P(1)O_4$ groups. Similarly, $Co(2)O_6$ octahedra share their apical oxygens O(6) and O(8) with $P(2)O_4$ tetrahedra. This arrangement would produce simple parallel chains extending in the [010] direction. However, the ''condensation'' of two of these chains by edge-sharing between the $Co(1)O_6$ octahedra and the $P(2)O_4$ tetrahedra (which share the edge O(7)–O(5)) and between $Co(2)O_6$ octahedra and $P(1)O_4$ tetrahedra (which share the edge O(1)–O(4)) leads to the formation of double chains. As a consequence of this arrangement two types of P–O bonds are found in the monophosphate groups: those corresponding to oxygen atoms involved in edge-sharing with CoO_6 octahedra are larger than those corresponding to corner-sharing. In contrast, the edges shared with CoO_6 octahedra are shorter than the others (see Table 4), the O(1)–P(1)–O(4) and O(5)–P(2)–O(7) angles being more acute than those corresponding to an ideal tetrahedron. The edge- and corner-sharing between phosphate groups and metal-containing octahedra is quite unusual (3); it is mainly limited to anhydrous phosphates of divalent transition metals such as $Co_3(PO_4)_2$

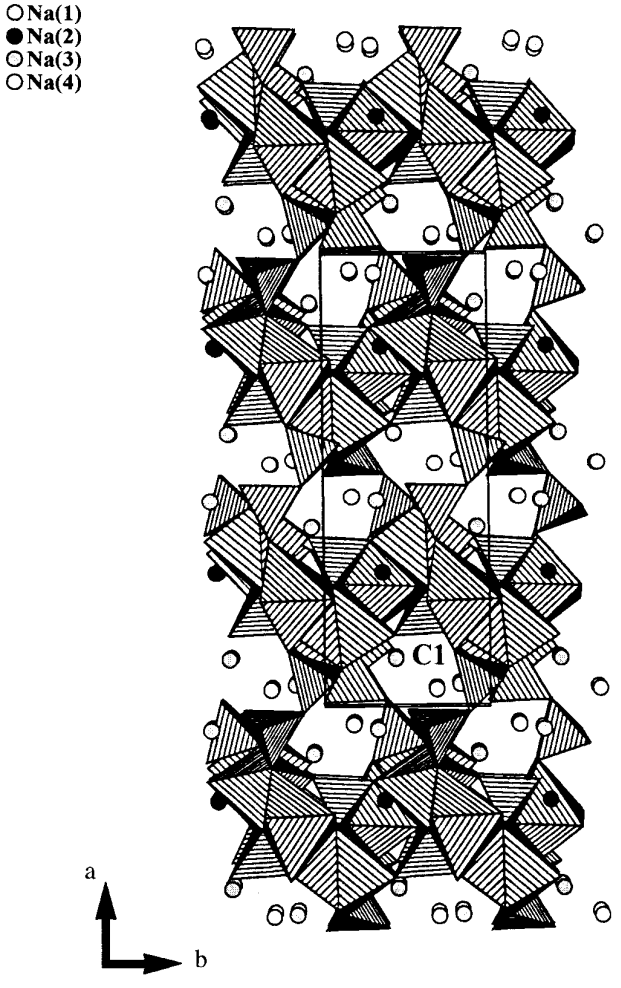

FIG. 2. Polyhedral view along the [001] direction of $Na_4Co_3(PO_4)_2P_2O_7$ showing one kind of channels C1.

(4). Extending along the [010] direction, in between two consecutive chains, a row of very distorted octahedral holes is formed. These holes are occupied by Co(3), as Fig. 3b shows. This may account for the quite irregular environment found for those atoms. As shown in Fig. 4, the $Co(3)O_6$ octahedra share the O(5)–O(14) edge with one $Co(1)O_6$ octahedron and the O(7) atom with another $Co(1)O_6$ octahedron. Besides, each $Co(3)O_6$ octahedron shares two apical oxygens (O(4) and O(1)) with two different $Co(2)O_6$ octahedra. As a result of this arrangement, a $(Co_3P_2O_{13})_\infty$ layer can be described as built up from two intersecting zig-zag chains of CoO_6 octahedra: one extending along the [0, 1, −1] direction, with a sequence $-Co(1)O_6-Co(3)O_6-Co(1)O_6-$ and the other running along the [0, 1, 1] direction, showing a sequence $-Co(2)O_6-Co(3)O_6-Co(2)O_6-$. Both chains intersect at the $Co(3)O_6$ octahedra. The $Co(1)O_6$ and $Co(2)O_6$ octahedra are linked along the *b* axis by PO_4 groups.

Two of these above described layers are joined along the *a* axis by pyrophosphate groups in such a way that large tunnels extending along the [010] and [001] directions occur between two neighboring sheets. In Fig. 1 it can be observed that two types of tunnels are formed in the [010] direction: one centered at (0, *y*, 0) (denoted as B1 hereafter) and another at (0, *y*, 1/2) (denoted as B2). Although both tunnels show a 6-ring window as viewed along the *b* axis, it must be recalled that octahedra and tetrahedra defining both B1 and B2 tunnels are, in fact, helically arranged. This means that, strictly speaking, the rings are not such. As can be seen in Figs. 5a and 5b, the size of the window of the B1 channel is clearly larger than that corresponding to the B2 tunnel.

On the other hand, only one kind of tunnel is formed along the [001] direction (denoted as C1 in Fig. 2) showing an irregular 7-ring window as viewed in the [001] direction. As is displayed in Fig. 5c, tetrahedra and octahedra defining this window are, like in B1 and B2 tunnels, helically arranged.

It is worth noting that there are also channels along the [100] direction (labeled by A1) crossing the $(Co_3P_2O_{13})_\infty$ layers (Fig. 6) and centered at (x, ≈1/4, ≈1/4). The shape and size of the corresponding 6-ring window (as viewed along the *a* axis) is drawn in Fig. 5d.

Interestingly enough, a complex scheme of tunnel intersections has been found in the structure of $Na_4Co_3(PO_4)_2(P_2O_7)$. Thus, both types of tunnels extending along the [010] direction (B1 and B2) intersect those running along the [001] direction (C1) (this situation can be denoted by B1 × C1 and B2 × C1). This produces a two-dimensional channel system parallel to the *bc* plane and located in between two neighboring $(Co_3P_2O_{13})_\infty$ layers. The intersection of the C1 and the A1 tunnels (A1 × C1) gives rise to the formation of a very open structure with a three-dimensional system of interconnecting channels. To our knowledge there is no example of phosphates or related materials showing a similar network of large intersecting tunnels. Very recently Harrison *et al.* (23) have reported the synthesis and structure determination of $K_2Nb_5GeO_{16}\cdot 2H_2O$ which contains a two-dimensional channel network. It is noticeable that the projection of this structure onto the (010) plane is quite similar to that of the title material along the [100] direction (Fig. 6). However, the polyhedral connectivity in both compounds is rather different and gives rise to important structure differences.

These tunnels host four crystallographically distinct sodium atoms. The Na(2) atoms are located into the A1 channel at the height of the $(Co_3P_2O_{13})_\infty$ sheet (see Figs. 1 and 2) and can be considered, to some extent, as a part

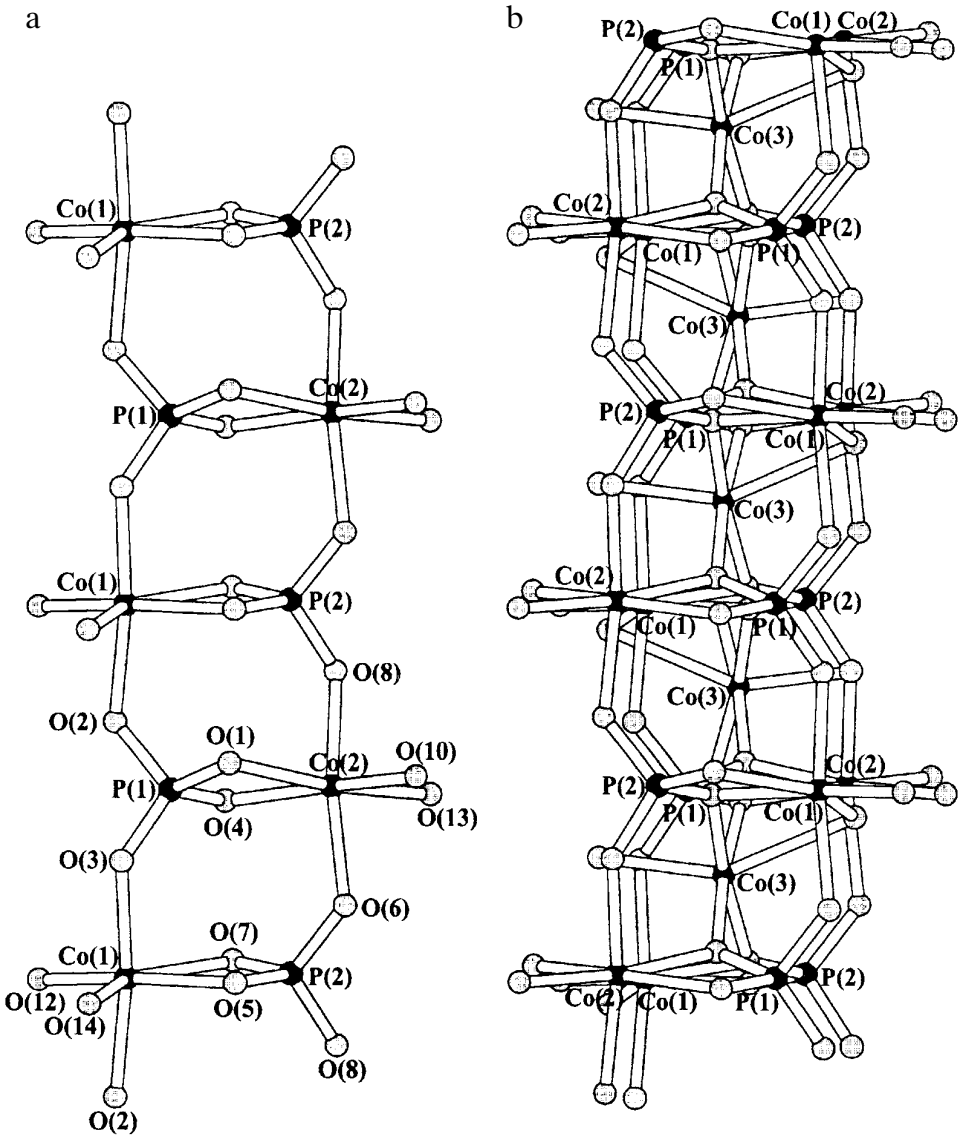

FIG. 3. (a) Representation of the double chains $[(Co(1)O_6–P(2)O_4)–(Co(2)O_6–P(1)O_4)]_\infty$ showing the corner- and edge-sharing scheme. (b) In between two double chains a row of octahedral sites occupied by Co(3) atoms occurs.

of that layer. In contrast, the rest of the sodium atoms are located at the intersection of two tunnels: Na(1) at B2 × C1, Na(3) at A1 × C1, and Na(4) at B1 × C1. This is clearly shown in Figs. 1, 2, and 6.

Taking into acocunt the very open framework of $Na_4Co_3(PO_4)_2(P_2O_7)$ and the location of the sodium ions at the intersecting large tunnels, this material should be a good ionic conductor. In other tunnel-containing materials which are good ionic conductors (24) the amplitude of thermal vibration of the sodium ions in the direction of the tunnels is associated with unhindered motion of those cations and with high ionic conductivity. However, as shown in Table 3, the anisotropic thermal parameters of the four sodium atoms are not larger than usual. Moreover, there is no direction along which the thermal motion of these ions is specially large. This can be explained by the stoichiometric nature of this compound; consequently the tunnels are ''filled up'' by sodium ions. This may produce strong electrostatic interactions between sodium cations occupying the same tunnel which would be responsible for the limitation of their mobility. Thus, the title compound, in spite of having a very open structure with Na^+ ions located at large channels, is expected to show low ionic conductivity. In this connection it is worth pointing out that in many compounds (25) a partial removal of sodium favors the mobility of the remainder cations and the ionic conductivity of the material is improved.

Besides the potential use of this material as a solid elec-

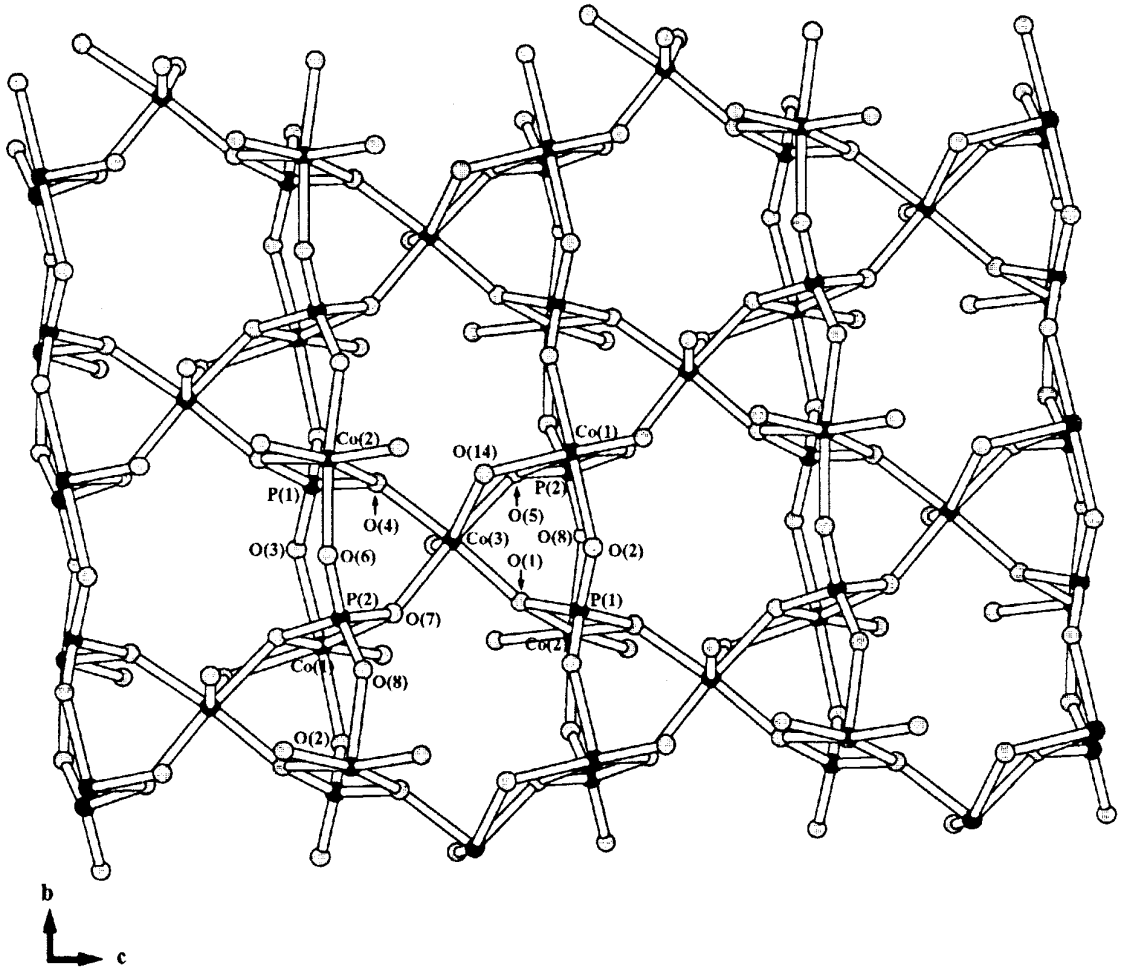

FIG. 4. Representation of one $(Co_3P_2O_{13})_\infty$ layer showing the corner- and edge-sharing scheme between CoO_6 octahedra and PO_4 tetrahedra.

trolyte, the connectivity of the CoO_6 octahedra in a $(Co_3P_2O_{13})_\infty$ layer (see Fig. 4) involving corner- and edge-sharing is expected to produce strong magnetic interactions between cobalt cations. Since two consecutive layers are separated by pyrophosphate groups, the distance between cobalt ions of neighboring layers is as large as $\approx a/2$ (9.023 Å). Thus, no or weak interlayer interactions are expected, which would yield a two-dimensional magnetic compound.

A deeper study of these interesting properties of the new and promising material $Na_4Co_3(PO_4)_2(P_2O_7)$ is in progress.

CONCLUDING REMARKS

The new compound $Na_4Co_3(PO_4)_2(P_2O_7)$ is an example of a mixed transition-metal phosphate showing some interesting structural features.

The main feature of this material is the existence of infinite layers parallel to the *bc* plane built up from CoO_6 octahedra and PO_4 tetrahedra which are connected along the *a* axis by pyrophosphate groups. Extending along the [010], [001], and [100], large tunnels occur within which the sodium ions are located. A complex scheme of tunnel intersections gives rise to a three-dimensional channel system.

The potential use of the title compound as a solid electrolyte is apparent. Besides, the structure of $Na_4Co_3(PO_4)_2(P_2O_7)$ should favor magnetic interactions between cobalt ions and, consequently, interesting magnetic properties are expected.

ACKNOWLEDGMENTS

We thank CICYT (Projects MAT-92-0374 and MAT-95-0809) for financial support. We express our gratitude to Mr. F. Rojas and Dr. R. Sáez-Puche for their help in the magnetic susceptibility measurements. We thank the staff of C.A.I. de Espectroscopía de Plasma, Universidad Complutense de Madrid, for chemical analysis.

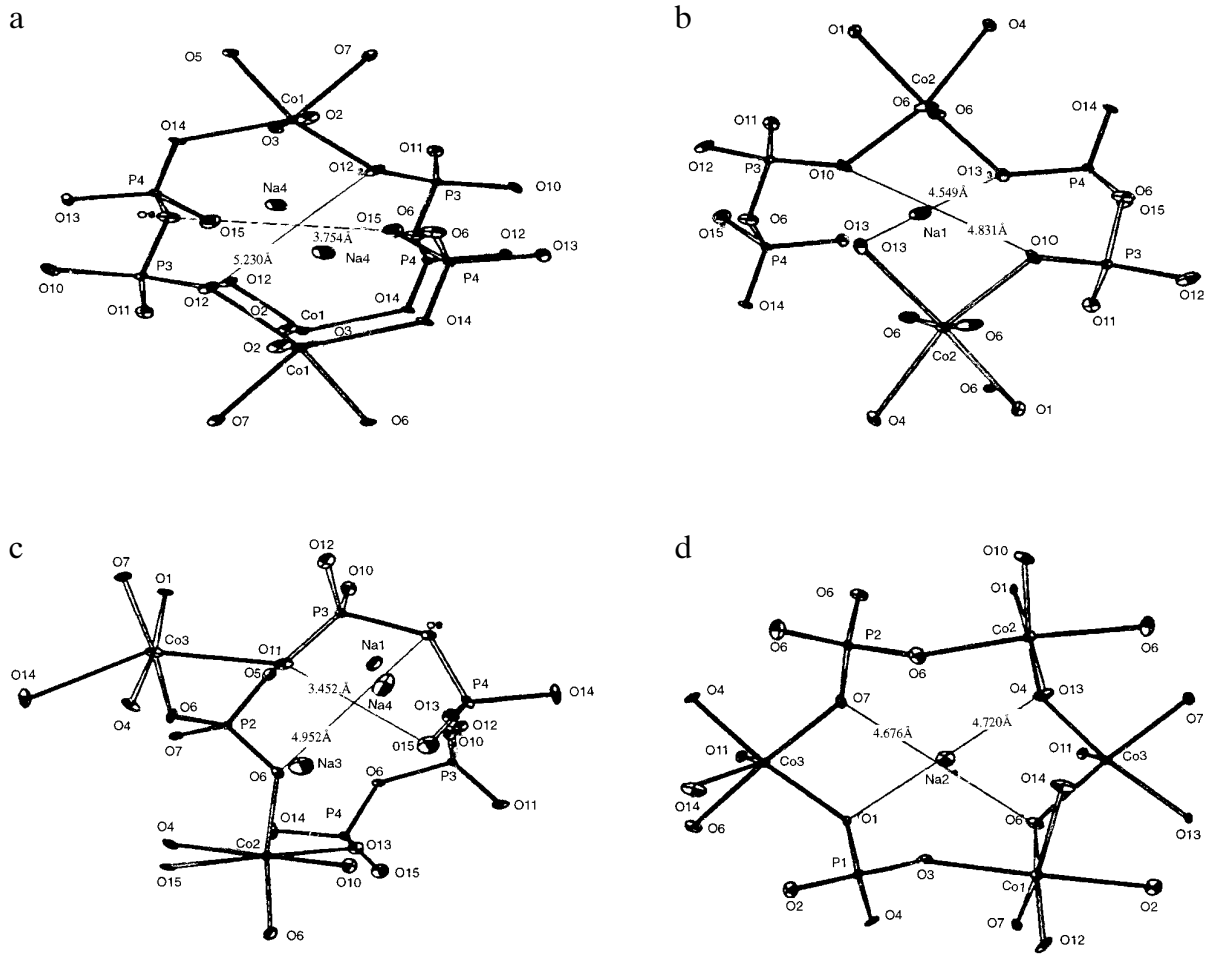

FIG. 5. ORTEP view of the shape and size of the free windows corresponding to the four different kinds of tunnels present in the structure of $Na_4Co_3(PO_4)_2P_2O_7$: (a) The polyhedra which define the 6-ring window of B1 are helically arranged. (b) The 6-ring window of B2 is not such, the octahedra and tetrahedra defining it are, like in B1, helically arranged. (c) Like in B1 and B2, the irregular 7-ring window of C1 is determined by polyhedra which are helically arranged. (d) The only window which is defined by polyhedra arranged in a ring is that corresponding to the A1 tunnels.

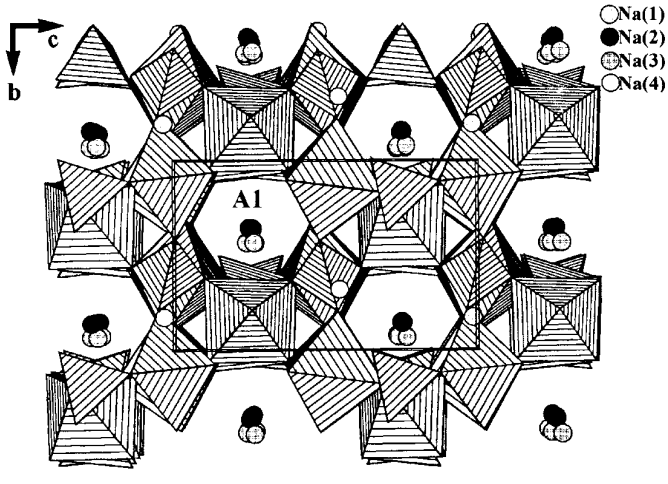

FIG. 6. Polyhedral view along the [100] direction of $Na_4Co_3(PO_4)_2P_2O_7$ showing the A1 channels.

REFERENCES

1. M. M. Borel, M. Goreaud, A. Grandin, Ph. Labbé, A. Leclaire, and B. Raveau, *Eur. J. Solid State Inorg. Chem.* **28,** 93 (1991).
2. P. Hong, *Mater. Res. Bull.* **11,** 173 (1976).
3. F. A. Ruszala, J. B. Anderson, and E. Kostiner, *Inorg. Chem.* **16(9),** 2417 (1977).
4. J. B. Anderson, E. Kostiner, M. C. Miller, and J. R. Rea, *J. Solid State Chem.* **14,** 372 (1975).
5. J. L. Pizarro, G. Villeneuve, P. Hagenmuller, and A. LeBail, *J. Solid State Chem.* **92,** 272 (1991).
6. H. Effenberger, *Acta Crystallogr. Sect. C* **48,** 2104 (1992).
7. K. H. Lii and P. F. Shih, *Inorg. Chem.* **33(14),** 3029 (1994).
8. W. Harrison, J. T. Vaughey, L. Dussack, A. Jacobson, T. Martin, and G. Stucky, *J. Solid State Chem.* **114,** 151 (1995).
9. D. Riou, P. Labbe, and M. Goreaud, *C.R. Acad. Sci. Paris,* Série II **307,** 1751 (1988).
10. R. E. Marsh, *Acta Crystallogr. Sect. C* **46,** 2497 (1990).
11. P. Lightfoot, A. K. Cheetham, and A. W. Sleight, *J. Solid State Chem.* **85,** 275 (1990).
12. S. Gali, K. Byrappa, and G. S. Gopalakrishna, *Acta Crystallogr. Sect. C* **45,** 1667 (1989).

13. F. Erragh, A. Boukhari, B. Elouadi, and E. M. Holt, *J. Cryst. Spectrosc. Res.* **21(3),** 321 (1991).
14. N. Krishamachari and C. Calvo, *Acta Crystallogr. Sect. B* **18,** 2883 (1972).
15. "International Tables for X-Ray Crystallography" Vol. **IV,** p 72. Kynoch Press, Birmingham, UK, 1974.
16. P. Main, S. J. Fiske, S. E. Hull, L. Lessinger, G. Germain, J. P. Declercq, and M. M. Woolfson, "MULTAN80, A System of Computer Programs for the Automatic Solution of Crystal Structures from X-ray Diffraction Data." Univ. of York, England, 1980.
17. N. Walker and D. Stuart, *Acta Crystallogr. Sect. A* **39,** 158 (1983).
18. M. Martínez-Ripoll and F. H. Cano, PESOS program. Instituto Rocasolano, C.S.I.C., C/Serrano 119, E-28006, Madrid, Spain.
19. J. M. Stewart, "The X-RAY80 System." Computer Science Center, University of Maryland, College Park, MD, 1980.
20. R. D. Shannon, *Acta Crystallogr. Sect. A* **32,** 751 (1976).
21. F. E. Mabbs and D. J. Machin, "Magnetism and Transition Metal Complexes" p. 20. Ed. William Clowes & Sons Limites, London, 1973.
22. D. W. J. Cruikshank, *J. Chem. Soc.* 5486 (1961).
23. W. T. A. Harrison, T. E. Gier, and G. Stucky, *J. Solid State Chem.* **115,** 373 (1995).
24. W. L. Roth, F. Reidinger, and S. J. LaPlaca, "Superionic Conductors" (G. D. Mahan and W. L. Roth, Eds.). Plenum Press, NY, 1976.
25. A. R. Wizansky, P. E. Rauch, and F. J. Disalvo, *J. Solid State Chem.* **81,** 320 (1989).